Effects of the molecular potential on coexcitations of valence electrons in the *K*-shell photoeffect of 3*p* and 4*p* elements

R. Hauko and J. Padežnik Gomilšek
Faculty of Mechanical Engineering, University of Maribor, Smetanova 17, SI-2000 Maribor, Slovenia

A. Kodre
Faculty of Mathematics and Physics, University of Ljubljana, Jadranska 19, SI-1000 Ljubljana, Slovenia and Jožef Stefan Institute, Jamova 39, SI-1000 Ljubljana, Slovenia

I. Arčon
University of Nova Gorica, Vipavska 13, SI-5000 Nova Gorica, Slovenia and Jožef Stefan Institute, Jamova 39, SI-1000 Ljubljana, Slovenia

G. Aquilanti
Elettra Sincrotrone Trieste, Trieste, I-34149 Basovizza, Italy

(Received 11 March 2019; published 3 June 2019)

Photoabsorption spectra of gaseous hydrides of 3*p* (PH_3, H_2S, HCl) and 4*p* elements (GeH_4, AsH_3, H_2Se, HBr) are measured in the energy region within 50 eV above the *K* edge, to study coexcitations of valence electrons by photoeffect in the *K* shell. The analysis of the valence coexcitations is extended to Ar, Kr, and SiH_4. Relative probabilities and energies of states in the individual coexcitation channels are recovered by modeling the spectral features with a minimal ansatz based on the features in the contiguous noble gas. The extracted parameters are compared to the results of theoretical calculations for molecules (ORCA code) and free atoms (Hartree-Fock code). The experimental results confirm that the valence coexcitations in the 3*p* and 4*p* hydride molecules can be satisfactorily described by a two-step process, with the shake of the outer electron following the excitation of the core electron. The total probability—relative to the *K*-edge jump—of the shake-up processes shows a steady decrease from 19% in Si to 14% in Cl, and from 15% in Ge to 12% in Br. The experimental values for Ar (12%) and Kr (10%) are in accord with the trend. The dominant contribution is the transition to quasiatomic orbitals, in contrast with the deeper coexcitation channels in hydride molecules where transition to molecular orbitals prevails.

DOI: 10.1103/PhysRevA.99.062501

I. INTRODUCTION

The smooth energy dependence of the x-ray absorption coefficient above a major absorption edge of an element is modified by small spectral features of two unrelated origins. One is a continuous oscillatory structural signal (XAFS: x-ray absorption fine structure) due to scattering of the photoelectron on the molecular or solid-state neighborhood of the atom [1]. The other consists of distinct groups of sharp features stemming from multielectron photoexcitations (MEPEs)—the coexcitations, in formation of the deep vacancy, of valence or core electrons due to correlated motion of the electron cloud. The structural signal is prevalent in aggregated samples of the element [2–6], and absent in samples of free atoms such as noble gases or vapors of metallic elements [3,7–15]. In these, MEPE can be studied directly, charting the energies of resonant collective excitations of the atom or the thresholds to successive ionization channels, as they are opened with the increasing photon energy.

In a theoretical description, the constituents of MEPE are attributed to a transition from the ground state of the atom to an excited or ionized state labeled by a specific configuration or rather a combination of configurations, mixed in by the correlation [16,17]. The MEPE groups can satisfactorily, but not exactly, be denoted by the dominating coexcited subshell, since the subshell binding energies are the prevailing contribution to the excitation energy: Thus, the groups appear in the absorption spectrum as separated features in the order of binding energies of consecutive subshells in the subsequent atom (the "$Z + 1$" rule).

The free-atom state is practically accessible only for a few elements [2,3,7–16,18–20]. The nonmetallic elements, in particular, remain—with the exception of iodine—in a molecular vapor to very high temperatures. In some of these elements another simple chemical form can be studied—a gaseous hydride, the atom with one to four hydrogen ligands. The structural signal, generated by the light ligands, is weak and simple, dominated by a single harmonic component: It can easily be simulated and removed from the absorption spectrum [21]. The basic effect of the H ligands to the electronic cloud is the formation of molecular orbitals, some occupied and some free. The unoccupied molecular orbitals are analogous to the valence orbitals in free atoms, but they open the possibility of additional MEPE transitions.

In the study of MEPE an interplay of experiment and theory is necessary. The measured x-ray absorption (XAS) spectra are the definite source of basic atomic data on correlation: However, the details of the MEPE features are smeared by the finite lifetime width of the core vacancy, so that the theoretical results, even those of simple self-consistent models, are helpful in identification of individual channels. In reverse, the experimental results provide a quantitative test of the more advanced models [8,14]. An important improvement in both aspects, the identification and the test, is gained with a combined analysis of data of related groups of elements: Along a series of consecutive elements [4,19–22], in our case the series filling the np subshell, the step-by-step development of MEPE features can be followed up to the canonical case of the noble gas, well studied and understood for the simplicity of its closed-shell structure. In another aspect, the degree of similarity of the valence-shell configurations in homologues, when established, can be used for interpretation of MEPE by corresponding sharper features in the spectrum of the lighter homologue [17,18,23].

We have measured photoabsorption spectra of gaseous hydrides of the elements in the $3p$ series (PH_3, H_2S, HCl) in the K-edge region. In an earlier experiment, devoted to deep coexcitations, the homologous $4p$ series (GeH_4, AsH_3, H_2Se, HBr) has been studied together with the corresponding noble gases Ar and Kr [17,21].

In a recently published analysis of $3p/4p$ edge structures [23], resulting from single-electron excitations, the $3p$ series has been completed by adoption of the data on SiH_4 [24], inaccessible in our experiment. The analysis has been extended also to spectra of $2p$ series hydrides (CH_4, NH_3, H_2O, HF) [25,26] and Ne [27]. The relative energies and probabilities of $1s$ electron transition to accessible bound states for homologous $3p/4p$ elements are quite similar, while transition parameters in $2p$ elements with a stronger prevalence of nuclear potential differ substantially. The measured spectra and molecular calculations testify to a strong influence of the molecular symmetry on the excitations into the lowermost unoccupied molecular orbitals, while the transitions to the higher quasiatomic orbitals remain largely unaffected, with the overall transition rate close to that of the adjacent noble gas.

The molecular reorganization of the valence levels is a major influence also in the coexcitation of the outer electrons—the valence MEPE, the subject of the present study. The fingerprints of the valence MEPE span the spectral interval of ~70 eV above the edge. For comparison with theory, the orbitals comprising the ground state and excited or ionized states of the hydride molecules are constructed by density functional theory (DFT) calculations in a self-consistent description in the molecular ORCA code [28]. The basic test is performed by the comparison of the calculated splitting of valence energy levels with the experimental results.

The relevant physical parameters of the coexcitations—relative photoexcitation probabilities and relative energies of states in the individual channels—are recovered by modeling the MEPE spectral features with a minimal ansatz based on the features in the contiguous noble gas. The extracted parameters are compared to the results of theoretical calculations for molecules (ORCA code) and free atoms (Hartree-Fock code [29]).

TABLE I. K-edge energies [33] and K-shell lifetime widths [34] of $3p$ and $4p$ elements. Energies from different theoretical calculations may differ by as much as 10 eV in both series.

$3p$	Si	P	S	Cl	Ar
E (keV)	1.839	2.146	2.472	2.822	3.203
Γ (eV)	0.5	0.5	0.6	0.6	0.7
$4p$	Ge	As	Se	Br	Kr
E (keV)	11.103	11.867	12.658	13.474	14.326
Γ (eV)	2.0	2.1	2.3	2.5	2.8

II. EXPERIMENT

Absorption spectra of gaseous hydrides PH_3, H_2S, HCl were measured in the energy interval of −200 to 300 eV relative to the K edge, with energy resolution of the monochromator 0.3 eV, smaller than lifetime widths of $1s$ excitations (Table I), at the XAFS beamline of the Elettra synchrotron in transmission detection mode at room temperature [30]. From a small vial the hydride gases were synthesized into a plastic syringe and injected through the PVC wall of the absorption cell, designed for experiments at room temperature in the soft x-ray regime [23].

The XAS spectra of $4p$ homologue hydrides GeH_4, AsH_3, H_2Se, HBr, and Ar and Kr were measured in transmission mode at the BM29 beamline of ESRF in Grenoble and at the E4, X1.1, and P65 beamlines at DESY, Hamburg, in the energy interval of −200 to 1000 eV relative to the K edge (Table I), with energy resolution of about 1 eV. The experiments, together with the preparation of the substances and the specific construction of the absorption cell are described in more detail in Refs. [16,21,31]. A deconvolution procedure [32] is applied to the $4p$ series spectra to reduce the effective linewidths and bring them closer to those of the $3p$ series (Fig. 1).

The normalized K-shell cross section is extracted from the measured XAS spectra by extrapolation of the preedge cross section, whereby the contribution of higher shells is determined and removed. The remaining K-edge absorption is normalized to the edge jump following the standard convention in absorption spectrometry.

The normalized K-shell absorption cross section of the measured elements is shown in Fig. 1. The relative energy scale is used, with the origin at the ionization threshold energy determined in the preedge analysis as described in Ref. [23].

The prominent wide resonances below the edge in Figs. 1(a) and 1(b) correspond to the transition of the $1s$ electron into the unoccupied molecular orbitals. They are followed by sharper resonances due to transitions into higher quasiatomic orbitals, continuing to the ionization threshold [23]. The features above the edge in Figs. 1(c) and 1(d), the subject of the present study, are due to the coexcitation of valence electrons, again starting with transitions to the molecular orbitals. With these, the smooth interval in the noble gas extending from the edge to the lowermost MEPE feature, is largely filled. The width of the molecular features is distinctly larger than that of quasiatomic resonances. In each case, the spectra of MEPE in the two homologues are remarkably similar.

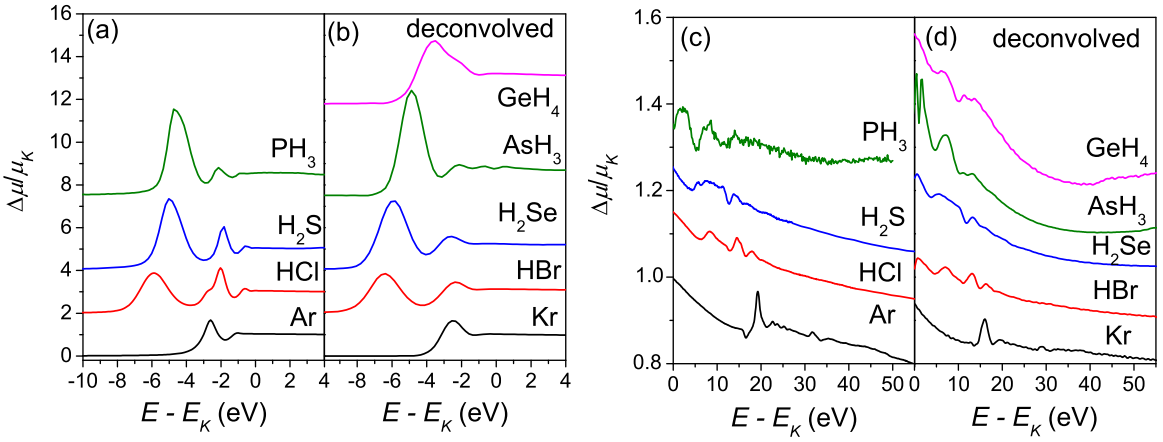

FIG. 1. The normalized K-shell absorption of hydrides of $3p$ (a),(c) and $4p$ elements (b),(d) after deconvolution, with respective noble gases. Below the edge (a),(b) the dominant feature is the wide resonant transition to the molecular orbitals, which is followed by sharper resonant transitions to quasiatomic orbitals; above the edge (c),(d) the MEPEs involving molecular orbitals precede the quasiatomic coexcitations. The spectra are displaced along the y axis for visibility.

III. METHODS

The extraction of the valence MEPE features from the normalized K-shell absorption spectra is a demanding operation even in the simple case of noble gases where the coexcitations of the closed-shell system are mostly well separated [see Figs. 1(c) and 1(d)].

Generally, each combined MEPE feature starts with a resonance resulting from the transition of both involved electrons into bound levels; it is followed by a tiny replica of an absorption edge resulting from the shake-up of the coexcited electron. Somewhat above the edge lies the threshold for double ionization (shake-off), recognizable only as a slight change of slope in the energy dependence of the cross section [16,17].

In noble gases, the resonant states in the individual channels are distinctly visible, and even the shake-up edges appear easily recognizable: superpositions of both, however, may present a problem. The changes of cross-section slope for the transition to the shake-off channels have long remained unresolved: They require an extremely careful modeling of the local course of the cross section, upon which a MEPE feature is superposed.

An increase of the absorption cross section immediately above the edge, steeply approaching the long-term power-law (Victoreen) trend [35,36] has already been observed in the early experiments on Ar [12]. In DFT calculations, a steep exponential decrease is explained by the postcollision interaction, the core polarization, and the virtual Auger processes [37–40]. In a recent theoretical study on K-shell photoabsorption on Ne the increase of the cross section above the edge is attributed also to the coherent interaction between single-electron and multielectron channels [41].

Following these explanations we introduced a heuristic exponential ansatz for the noble-gas cross section in the ∼20 eV interval between the top of the Rydberg series and the onset of first MEPE corresponding roughly to the binding energy of the lowest valence orbital in the $Z+1$ approximation [16,42], and used the fitted decay constant in modeling the hydride spectra.

The ansatz of the exponential baseline has been tested on the spectra of Ar (see Fig. 2) and deconvolved Kr [16]: The energy position and relative probability of the extracted resonances, and the shake-up and shake-off MEPE are shown in Table II. In spite of a simplified model including a modest number of channels, the result for the total shake probability in Ar (20%) agrees well with first-measured satellite intensities in high-resolution emission spectroscopy (∼30%) [12], the first theoretical calculations of double-photoexcitation cross section (∼18%) [43], as well as with other published data, including the latest emission-spectroscopy experiments [15,44–47]: In these, it is necessary to take into account the standard normalization of excitation probabilities for the transitions to the single-excitation channel, leading to ∼10% higher values for shake-up and up to 50% for shake-off channels in this energy region.

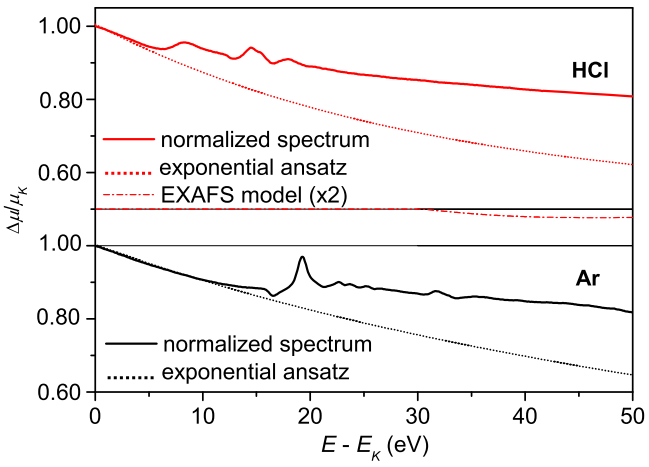

FIG. 2. The constituents of the normalized chlorine absorption cross section in HCl immediately above the K edge: the EXAFS signal of the hydrogen neighbor with amplitude up to 1% of the K-edge jump (dash-dot line), magnified and shifted vertically for clarity, and the exponential ansatz (dot line) for the smooth one-electron photoexcitation cross section. For comparison, the corresponding region in Ar is shown.

TABLE II. The MEPE energies and relative probabilities in Ar and Kr, with uncertainty estimates, used in modeling of the hydride spectra. The resonant-channel probabilities are given relative to the leading single-electron resonance $[1s](n+1)p$, and the transition probabilities for the shake channels are expressed relative to the K-edge jump. The probabilities in the second column refer to the summed contribution of shake-up to all Rydberg p orbitals.

	Final states	$[1snp](n+1)p^2$	$[1snp](n+1)p$	$[1snp]$	$[1sns](n+1)s(n+1)p$	$[1sns](n+1)s$
Ar	Rel. energy (eV)	19.3 ± 0.5	21.6 ± 0.5	31.1 ± 1.0	31.7 ± 1.0	34.1 ± 1.5
	rel. prob. (%)	11.8 ± 1.0	10.7 ± 1.0	7.6 ± 1.0	2.4 ± 0.5	1.4 ± 1.0
Kr	Rel energy (eV)	16.0 ± 0.5	18.2 ± 0.5	26.6 ± 1.0	29.3 ± 1.0	31.5 ± 1.5
	rel. prob. (%)	13.9 ± 1.0	8.6 ± 1.0	6.5 ± 1.0	2.9 ± 0.5	1.3 ± 1.0

In hydrides, as in molecular gases generally, MEPE features are further obscured by the weak XAFS signal: Its amplitude, up to 2.5% of the K-edge jump, is proportional to the number of hydrogen ligands (see Fig. 2), but remains practically negligible within the interval of interest.

In this work, the K-shell photoabsorption signal in the energy interval up to 50 eV relative to the K edge is treated as a sum of the heuristic exponential due to single-electron photoexcitation, the XAFS signal, and the MEPE signal. Since there is no "clear interval" above the edge with the low molecular orbitals filling the energy gap, the exponential ansatz with parameters for the adjacent noble gas can be used with good result (see Fig. 2). Further out from the edge, the local baseline of the cross section can be estimated from some theoretical calculations on hydrides [38] and those of the FEFF9 code in the XANES module [48].

The extracted contribution of the MEPE to the normalized K-shell absorption cross section in the $3p$ and $4p$ hydrides is shown in Fig. 3. As expected, the spectra are richer in number of excitation channels than those of noble gases. To unravel the complex features, resulting from strong overlap of states in the individual excitation channels, the similarity with noble-gas spectra is first used to extract the quasiatomic excitations, where both electrons are promoted to orbitals with prevailing atomic character or to continuum (see Fig. 5). Further, the group of molecular MEPEs is identified by using

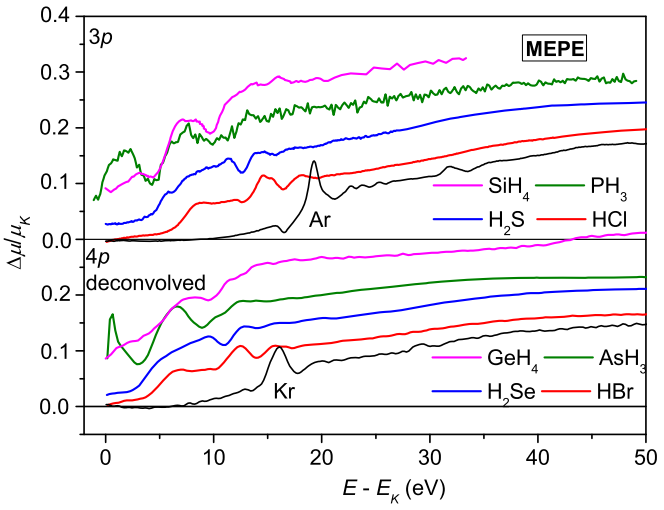

FIG. 3. The extracted valence coexcitations of the two hydride series and the adjacent noble gases, with SiH_4 spectrum, derived from [24]. Spectra are displaced vertically for visibility, top to bottom: SiH_4 to Ar and GeH_4 to Kr.

the results of molecular calculations and the data on single excitations to molecular orbitals, obtained from the edge profile [23]. The residual features are attributed to excitations to one quasiatomic and one molecular orbital.

In this work, the valence orbitals will be, for the sake of clarity, denoted by atomic symbols np and ns ($n = 3, 4$) with, if necessary, indication of symmetry in brackets; the unoccupied antibonding molecular orbitals will, regardless of symmetry, be denoted by σ^*. Valence spin-orbit splitting (up to 0.3 eV in the $4p$ series) is neglected.

Transition energies in free atoms were calculated with the HF86 code [24]. For hydrides, the nonrelativistic molecular DFT calculations were, as in Ref. [23], performed with the ORCA package, including the exchange-correlation potential BP86, a combination of the exchange functional from Becke in 1988 [49] and the correlation functional from Perdew in 1986 [50]. Inside frozen-core approximation with 10 ($3p$) and 18 ($4p$) frozen-core electrons, two sets of split-valence Gaussian base functions were used: the small and computationally efficient def2-SVP from the Ahlrichs group [51,52] primarily for the calculations of molecular orbital energies, and aug_cc_pV5(6)Z [53,54] of the Dunning group for transition probabilities, in accord with the experience from the below-edge study.

The MEPEs are treated as a two-step process, in sudden approximation. Such calculation is conventionally used for deeper coexcitations, but it agrees surprisingly well with satellite energies in a recently measured photoelectron spectrum of H_2S [55]. It also describes well the cross section $[1s3p]$ in Ar [56], agreeing perfectly with the latest many-body perturbation results [57]. In this approximation, the excited or ionized molecule configuration, built on the ground-state geometry, is adopted for the initial state. The core vacancy is, following the $Z+1$ approximation in molecular calculations, corrected for by an additional unit of charge at the central atom. The calculated energy levels in $3p$ hydrides with $[1s]$ vacancy are shown in Fig. 4. The $4p$ hydride graph is similar.

In this approximation, the threshold energies of shake-up and shake-off transitions—relative to the K edge—are estimated as electron promotion from the valence orbital to an unoccupied orbital or continuum in the ionized molecule with $[1s]$ core hole, while for resonant transitions into molecular orbitals $[1snp]\sigma^{*2}$, the initial state is taken as the state with an electron promoted from $1s$ to the lowermost free molecular orbital, and the final state as a state with additional promotion. The mixing of initial np states and all final states is included.

The final states involving one of the higher quasiatomic orbitals are introduced in the calculation step by step to ensure

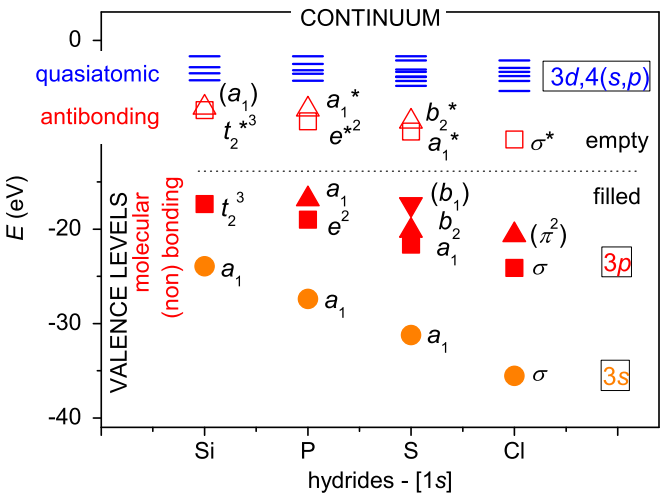

FIG. 4. Calculated energy levels in the $3p$ hydride molecules with a $[1s]$ vacancy, together with parent orbital labels of the central atom. Symmetry labels are given, with the degeneracy in the upper index and the nonbonding orbitals in parentheses.

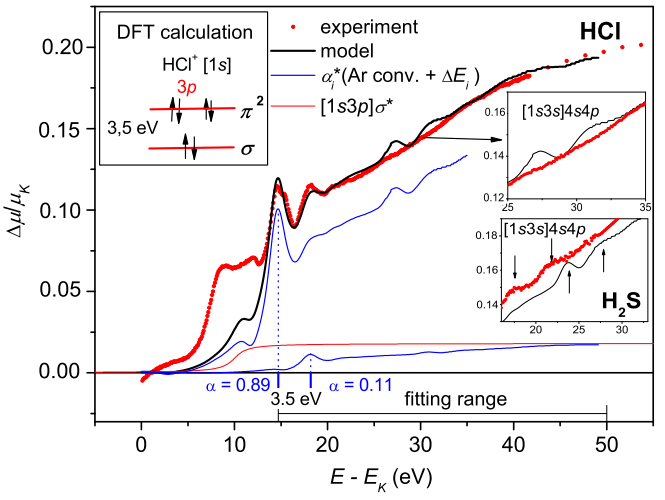

FIG. 5. Coexcitation spectrum of HCl. Experiment (red dots), the model of higher-energy part—quasiatomic coexcitations (black) and its components: the edge (red line), the shifted coexcitation spectra of Ar (blue line). The unmodeled low-energy part of the coexcitation spectrum corresponds to resonances involving the molecular orbitals. Insets: valence levels (left), the $3s$ coexcitation intervals of HCl and H_2S (right).

the stability of the procedure and to exclude "continuum orbitals." The procedure includes mixing of quasiatomic orbitals with the lower-lying molecular orbitals. In this way, total probability of resonant transitions into at least one molecular orbital is obtained (denoted "total" in Table III).

Some parameters in the calculation are adopted from the analysis in [23]: The relative energy of the lowermost free molecular orbital is used to estimate the shift of the calculated energy levels, and the probability for the excitation into the initial state of our calculation is factorized into the final probabilities result. The calculated relative probabilities are given in the H_2S probability units for convenience. Results are, together with the number of constituting transitions, shown in Table III. Estimates of the "mixed-resonance" probabilities are obtained as the difference of the probabilities of "total" and "molecular resonances" $[1snp]\sigma^{*2}$.

The analysis in Ref. [23] showed that—independently of the hydride series and of the symmetry of the molecule—inside the ORCA code, the molecular orbitals can be calculated with a better precision than the higher-lying quasiatomic orbitals. Consequently, in modeling of the MEPE features in hydride spectra we only used the calculated relative energies and probabilities for transitions to molecular orbitals.

A. Quasiatomic coexcitations

As evident from Fig. 4, the difference of the binding energies of the unoccupied molecular orbital and the higher quasiatomic orbitals, and accordingly the energy step between corresponding features in the MEPE spectra, increases with the nuclear charge in both series of molecules. In spectra of both halogene hydrides the coexcitations to the molecular and quasiatomic orbitals are well separated.

It is to be expected that the coexcitation processes to higher (quasiatomic) orbitals, almost unaffected by the molecular symmetry, should, at least in HCl and HBr, be similar to those in Ar and Kr, apart from the energy splitting in valence np levels which produces two series of transitions. The valence MEPE spectrum of HCl and the model of its high-energy part is shown in Fig. 5. The constituents of the model are (1) two copies of the Ar MEPE (with adapted linewidth) to account for the multiplet splitting in HCl, with total transition probability and energy as the variational parameters; and (2) a constant, describing the contribution of single ionization with coexcitation to the molecular orbital $[1snp]\sigma^*\varepsilon p$ in this region.

TABLE III. The calculated relative probabilities of double-electron transitions into unoccupied bound states, of which at least one is a molecular orbital, with number of transitions in brackets. The values are given relative to coexcitation to the molecular orbitals in H_2S, representing 2.3% of the measured sum of probabilities of the single-electron transition into the $[1s]\sigma^*$ states in H_2S.

$3p$	SiH_4	PH_3	H_2S	HCl
Mol. res. $[1s3p]\sigma^{*2}$	1.53 {24 trans.}	1.82 {18}	1.00 {12}	0.24 {6}
Mix. res. $[1s3p]\sigma^* n'l'$	0.52	1.35	1.33	1.03
total	2.05 {78}	3.18 {72}	2.33 {66}	1.27 {72}
$4p$	GeH_4	AsH_3	H_2Se	HBr
mol. res. $[1s4p]\sigma^{*2}$	1.88 {24}	2.20 {18}	1.23 {12}	0.33 {6}
mix. res. $[1s4p]\sigma^* n'l'$	0.62	1.41	1.65	1.24
total	2.50 {78}	3.62 {72}	2.88 {66}	1.57 {72}

The parameters of the model were determined by the LINEAR COMBINATION FIT option in the ATHENA code [58]. Both resonances and the region above are satisfactorily modeled. The coefficients pertaining to relative amplitudes of the noble-gas replicas in the linear combination add to a value close to unity, and the energy shift of the replicas is in agreement with the calculated energy difference of the valence levels in the ionized molecule.

In [23], the summed probabilities for the single-electron transitions to quasiatomic orbitals in hydrides were found essentially identical to the values for the noble gas at the end of the series. The same relation is expected for coexcitations and, furthermore, even for partial probabilities and partial energy shifts for coexcitations into the quasiatomic orbitals and/or the continuum. Therefore, the model, together with arctangent ansatz for shake-up, centered at the calculated threshold energy into the $[1snp]\sigma^*\varepsilon p$ final state, is used in all hydrides. Overall, good agreement is found, with the largest deviations in SiH_4 and GeH_4.

The modeling yields three independent parameters: the relative probability of the shake-up into the $[1snp]\sigma^*\varepsilon p$ states, the relative mean energy, and the summed relative probability of resonances into the $[1snp](n+1)p^2$ states. The full model description is reconstructed with the corresponding ratios in the pertinent noble gas: The shake-up and shake-off thresholds, respectively, are 2.3 and 10.7 eV above the resonance, and the sum of the amplitudes of noble-gas copies in the model is the multiplying factor of the probabilities in Table II.

Since our model ansatz for quasiatomic excitations is built on the np and ns MEPE data of Ar and Kr, the ns coexcitations in hydrides are not modeled properly. The effect on np parameters, obtained from the fit, is very small in view of the weak ns contribution. Figure 5 includes the detail of the HCl spectrum where $[1s3s]4s4p$ MEPE is expected but not observed. It can though be found in the H_2S spectrum (the second inset), ~7 eV lower than in the model, and in the remaining hydrides at energies which agree with the calculated values. The strength of the $3ns$ MEPE depends on the symmetry of the molecule: It is a monopole transition of the ns electron to the lowermost quasiatomic $(n+1)$ s orbital, modified in HCl and HBr by the linear geometry toward a p-like state, while gaining in sphericity in predecessor hydrides. The same effect has been observed in the preedge part of the spectrum where the forbidden free atom transitions into the $[1s](n+1)s$ state are recognized in spectra of linear HF, HCl, and HBr molecules.

B. Molecular coexcitations

From the analysis of quasiatomic coexcitations the probabilities of the shake-up transitions to molecular orbitals $[1snp]\sigma^*\varepsilon p$ are derived (see Fig. 5). The lowest spectral region of valence MEPE includes the resonances into the $[1snp]\sigma^{*2}$ final states with both electrons promoted to molecular orbitals (see Fig. 3). The energy is too low for other coexcitation channels, so the energies and an approximation for probabilities can be directly estimated from the MEPE spectra, with a subsequent refinement with results of molecular calculation.

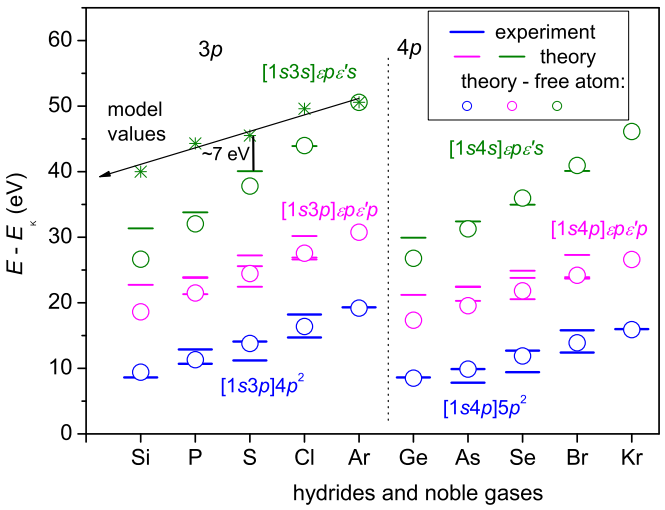

FIG. 6. The experimental values of relative energies above K-shell threshold of resonances into the $[1snp](n+1)p^2$ states (blue lines) and theoretical values of np (magenta) and ns (olive) double-ionization thresholds from molecular calculation. The Hartree-Fock energies for the free atom are shown by circles of respective colors. For H_2S, the estimated modeling error is indicated by a vertical line.

The calculated values for molecular resonances from Table III are adjusted for a best fit to the experimental MEPE spectra: A single value for the linewidth and a common amplitude factor are adopted for the resonances. Since they span a narrow interval of ~3 eV, a single resonant term with an adjusted width, placed at the centroid of the group, is sufficient—except for the cases of PH_3 and AsH_3 where, as indicated by calculations, two resonant terms are required in the model (see Fig. 8).

IV. RESULTS

In Fig. 6, the energies of quasiatomic resonances into the $[1snp](n+1)p^2$ states determined in modeling the spectra are shown relative to the K-shell threshold. For comparison, theoretical values from Hartree-Fock calculation for free atoms are given, together with values for Ar and Kr. As already established in [23], the molecular potential affects the lowermost $(n+1)p$ orbital hardly at all, the mean transition energies agreeing closely with Hartree-Fock values for the free atom.

Threshold energies for double ionization of the molecule into the $[1snp]\varepsilon p\varepsilon' p$ and $[1sns]\varepsilon p\varepsilon' s$ states, calculated with the molecular code and the Hartree-Fock code for free atoms in frozen-core approximation are also shown. Except in Si and Ge the values from both codes agree well. The experimental data provide a test of molecular calculations using the $Z+1$ approximation: The binding energy of a high orbital is proportional to the square of the effective charge for that orbital. For valence orbitals, the effective ion charge $Z_{\text{eff}} \sim 1$ is doubled with the formation of the core hole [59]. The difference of calculated $[1snp]$ and experimental $[1snp](n+1)p$ threshold energies in all hydrides is approximately fourfold energy of the $(n+1)p$ binding energy, i.e., the difference of $[1s]$ and $[1s](n+1)p$ thresholds reported in Ref. [23], as expected.

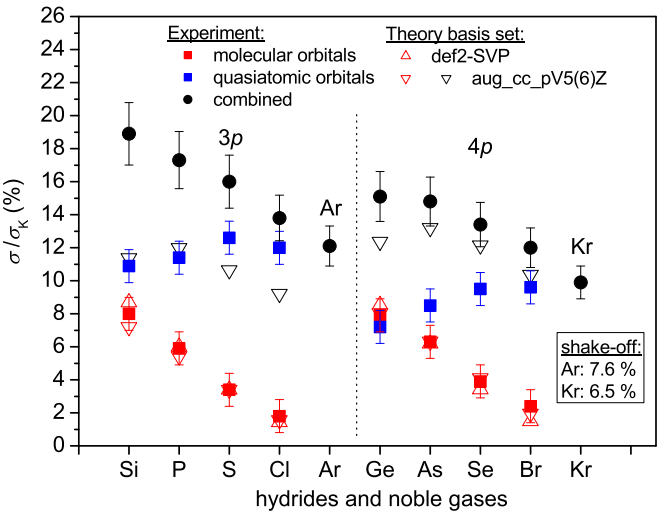

FIG. 7. The experimental total cross sections for shake-up of np or ns electron to a molecular orbital (red), a quasiatomic orbital (blue) and their sum (black), together with the theoretical values (empty symbols of corresponding color).

The shake-up relative probabilities in the energy region just above the threshold, obtained in modeling the measured spectra, are shown in Fig. 7: The processes, which lead to final configurations $[1sn(p,s)]n'(p,s)\varepsilon(p,s)$ and $[1sn(p,s)]\sigma^*\varepsilon(p,s)$ are included. The relative excitation probabilities of the individual states in the $[1sn(p,s)]\sigma^*\varepsilon(p,s)$ channels decrease along each atomic series in proportion to the number of accessible molecular orbitals. The individual relative values in the $4p$ series are on average 20% higher than in $3p$. The trend does not follow the dipolar single excitation to molecular orbitals where the symmetry of the molecule is the decisive factor. In the coexcitation, on the other side, the monopolar promotion of the valence electrons from bonding to antibonding molecular orbitals with equal symmetry is the main contribution to the cross section, which therefore depends more weakly on the geometry of the molecule.

The excitations to the quasiatomic orbitals are much stronger than those to the molecular orbitals: Both channels are comparably strong only in GeH_4 and AsH_3. The summed probability decreases slowly along the series toward the values of 12% and 10% for the respective noble gases. This is different from the deeper coexcitations into the $[1s3(p,s)]$ final states in $4p$ hydrides [21] and solid compounds [4], where the value is directly proportional to the number of free molecular orbitals. Evidently, valence coexcitations lead prevailingly to the quasiatomic levels, and the deeper coexcitations to the molecular orbitals.

For comparison, the calculated values are shown, normalized to the measured H_2S value; for shake-up to molecular orbitals $[1sn(p,s)]\sigma^*\varepsilon(p,s)$, both base-function sets give almost identical results with a good agreement with experimental values for all other hydrides. For the total shake-up probabilities, the trend with atomic number follows the experiment well, but individual values agree less well. The strong mixing in the initial configuration increases the calculation uncertainty of the coexcitation of the ns electron, contributing

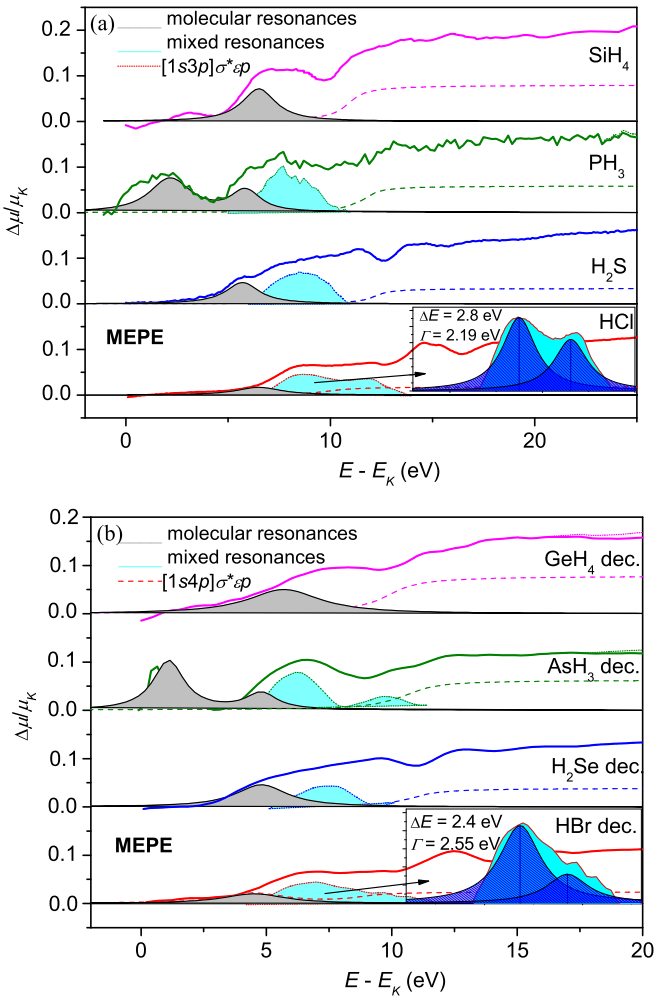

FIG. 8. Modeling the lower part of the MEPE spectrum (solid curve) for the $3p$ (a) and the deconvolved $4p$ series (b) includes resonant transitions into the $[1sn(p,s)]\sigma^{*2}$ final states (gray area) and shake-up into the $[1sn(p,s)]\sigma^*\varepsilon(p,s)$ final states (area under the dashed line). The residual (turquoise area) is attributed to the mixed-resonant channels. In the transparent insets, the model of mixed resonances in HCl and HBr, described in the text, is shown.

10%–15% of the total shake-up. The same monotonic trend inside both series is found in theoretical calculations of total shake probabilities for free atoms [60,61].

The dominance of coexcitation to the atomic orbitals is found also in an emission-spectroscopy experiment on H_2S [55]. The experimental and theoretical probabilities for transition into the $[1s2p]\sigma^*\varepsilon p$ states in H_2O [62] are given in the range of 2.6%–3.4%, comparable to our results for homologous hydrides H_2S (3.4% $\pm$ 1.0%) and H_2Se (3.9% $\pm$ 1.0%).

The model contribution of the coexcitation from np into bound states with at least one molecular orbital is shown in Fig. 8. The lowest MEPE features are similar for all homologue pairs. A slight deviation of the two-step model cross section from the measured values can be noticed. For the resonant excitations to molecular orbitals, the ratio of the total probabilities of double to single transitions is close to the ratio of the edge jumps for transitions into the $[1sn(p,s)]\sigma^*\varepsilon(p,s)$ and $[1s]\varepsilon p$ states in all elements, shown in Fig. 7.

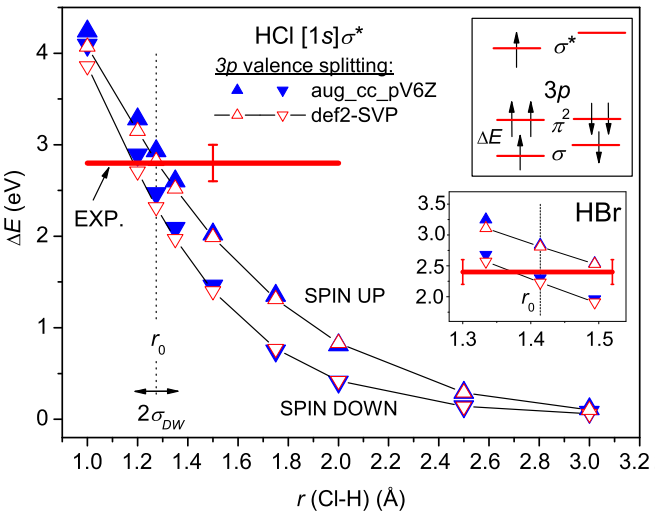

FIG. 9. HCl [1s]σ^* valence splitting, calculated as a function of interatomic distance. Spin interaction yields two values for each distance (inset). For comparison, the measured energy difference of the two mixed resonances is shown, with an estimate of its possible error. The mean interatomic distance r_0 and the Debye-Waller factor σ_{DW} are also shown. In HBr (lower inset) a similar pattern is observed.

The mixed resonances, prominent in HCl and HBr, are practically absent in SiH_4 and GeH_4. The values, obtained as residuals, are subject to a large ∼20% error. The attribution of the mixed resonances into the $[1snp]\sigma^* nl$ states in Fig. 8 is in part arbitrary, but in the simplest case of HCl and HBr a supportive argument can be given: The model of two resonant terms pertaining to transitions from np orbitals with different symmetry into the $[1snp(\pi^2)]\sigma^*(n+1)p$ and $[1snp(\sigma)]\sigma^*(n+1)p$ final states yields the energy splitting and the widths in good agreement with the results of calculation and of the analysis of single excitation in Ref. [23] (insets in Fig. 8).

The mixed-resonance amplitudes, determined in the modeling and normalized to the probability of the single-electron transition $[1s]\sigma^*$ i.e., the first step of the two-electron transition, increase in both series of hydrides, and so do the ionization energies of the parent np orbitals. The maximum ionization energies (in Cl and Br) are close to the ionization energy of the H atom, making the ground state of HCl and HBr molecules the most tightly bound in the series, and their excited $[1s]\sigma^*$ states most prone to dissociation [63]. This might lead to a conjecture that the shake of the valence electron coincides with the breaking of the excited molecule, but a comparison of the calculation and the experiment shows the contrary: While the H-Cl distance in the theoretical model increases from the equilibrium value 1.27 Å toward 3.0 Å, the splitting of the valence levels, the transition energies, and probabilities all decrease, the values at larger distances being in evident disagreement with experiment (see Fig. 9). The same is true for HBr. Hence we conclude that the shake of the valence electron takes place in the geometry of the ground-state molecule.

Generally, the disagreement in both homologue series between the measured MEPE spectra and the model increases with the number of H ligands, or, in other words, the sphericity of the molecule, reaching a maximum with SiH_4 and GeH_4. In this way, the contribution of the triple-electron excitation into the $[1snp^2]\sigma^{*3}$ final states, not included in the model, is estimated in SiH_4 and GeH_4 as ∼50% of the double-electron process into the $[1snp]\sigma^{*2}$ states or ∼3% of the direct excitation into the $[1s]\sigma^*$ states. The contribution is hardly observed in the subsequent elements, P and As, and remains hidden in the other spectra in the series.

V. CONCLUSIONS

The joint analysis of two homologue series yielded a reliable identification of valence coexcitations with estimates of transition probabilities and energies, and a comparison with theoretical results of molecular ORCA and atomic Hartree-Fock codes. The MEPE features in homologue pairs are similar in shape, testifying to the similarity of the valence-shell configuration with minimum influence of the closed shells below.

The experimental results confirm that the valence coexcitations in the $3p$ and $4p$ hydride molecules can be satisfactorily described by a two-step process, with the shake of the outer electron following the excitation of the core electron. Within the experimental (or analytical) uncertainty no effect of coherent excitation of the two electrons can be recognized.

The influence of the molecular potential to valence excitations is weak; the electron correlations are independent of the symmetry of the molecule. In comparison to the free-atom case, only the channels involving coexcitation into molecular orbitals are modified to some extent. The discrete symmetry of the molecule leaves an imprint on MEPE through the specific multiplet splitting of the energy levels.

The total probability—relative to the K-edge jump—of the shake-up transitions into the $[1sn(p,s)]n'(p,s)\varepsilon(p,s)$ and $[1sn(p,s)]\sigma^*\varepsilon(p,s)$ final states shows a steady decrease from 19% in Si to 14% in Cl, and from 15% in Ge to 12% in Br. The experimental values for Ar (12%) and Kr (10%) are in accord with the trend. The dominant contribution is the transition to quasiatomic orbitals, in contrast with the deeper MEPE in hydride molecules, where coexcitations to molecular orbitals prevail.

The analysis of the resonant coexcitations, inaccessible in electron-emission spectroscopies, gives evidence that the coexcitation takes place in the ground-state geometry of the HCl and HBr molecules.

ACKNOWLEDGMENTS

We acknowledge access to the SR facilities of ELETTRA (beamline XAFS, Proposals No. 20150107 and No. 20115112), ESRF (beamline BM29, Proposal No. HE-375), and DESY, a member of the Helmholtz Association (HGF) (beamlines X1 Proposals No. II-98-043 and P65 No. I-20180356 EC). Luca Olivi (ELETTRA), and Larc Troeger and Edmund Welter (DESY) provided expert advice on beamline operation. The research was supported by the Slovenian Research Agency (P1-0112), and partly by the project CALIPSOplus under the Grant Agreement No. 730872 from the EU Framework Programme for Research and Innovation "HORIZON 2020."

[1] J. J. Rehr and R. C. Albers, Rev. Mod. Phys. **72**, 621 (2000).
[2] A. Kodre, J. Padežnik Gomilšek, A. Mihelič, and I. Arčon, Radiat. Phys. Chem. **75**, 188 (2006).
[3] A. Kodre, I. Arčon, and J. Padežnik Gomilšek, in *International Tables for Crystallography* (IUCr, in press), Vol. I, Chaps. 8.1 and 3.23.
[4] J. P. Gomilšek, A. Kodre, I. Arčon, A. M. Loireau-Lozac'h, and S. Benazeth, Phys. Rev. A **59**, 3078 (1999).
[5] J. Padežnik Gomilšek, A. Kodre, I. Arčon, S. de Panfilis, and D. Makovec, J. Synchrotron Radiat. **18**, 557 (2011).
[6] J. P. Gomilšek, I. Arčon, S. de Panfilis, and A. Kodre, Phys. Rev. A **79**, 032514 (2009).
[7] J. P. Gomilšek, A. Kodre, I. Arčon, and M. Hribar, Phys. Rev. A **68**, 042505 (2003).
[8] A. Kodre, J. Padežnik Gomilšek, I. Arčon, and G. Aquilanti, Phys. Rev. A **82**, 022513 (2010).
[9] A. Mihelič, A. Kodre, I. Arčon, J. Padežnik Gomilšek, and M. Borowski, Nucl. Instrum. Methods Phys. Res., Sect. B **196**, 194 (2002).
[10] A. Filipponi, L. Ottaviano, and T. A. Tyson, Phys. Rev. A **48**, 2098 (1993).
[11] J. P. Gomilšek, I. Arčon, S. de Panfilis, and A. Kodre, J. Phys. B **41**, 025003 (2008).
[12] R. D. Deslattes, R. E. LaVilla, P. L. Cowan, and A. Henins, Phys. Rev. A **27**, 923 (1983).
[13] J. M. Esteva, B. Gauthe, P. Dhez, and R. C. Karnatak, J. Phys. B **16**, 263 (1983).
[14] I. H. Suzuki and N. Saito, J. Electron. Spectrosc. Relat. Phenom. **129**, 71 (2003).
[15] M. Kavčič, M. Žitnik, K. Bučar, A. Mihelič, M. Štuhec, J. Szlachetko, W. Cao, R. Alonso-Mori, and P. Glatzel, Phys. Rev. Lett. **102**, 143001 (2009).
[16] A. Kodre, I. Arcon, J. Padeznik Gomilsek, R. Preseren, and R. Frahm, J. Phys. B **35**, 3497 (2002).
[17] J. P. Gomilšek, A. Kodre, I. Arčon, and R. Prešeren, Phys. Rev. A **64**, 022508 (2001).
[18] J. Padežnik Gomilšek, A. Kodre, I. Arčon, and G. Bratina, Phys. Rev. A **84**, 052508 (2011).
[19] U. Arp, B. M. Lagutin, G. Materlik, I. D. Petrov, B. Sonntag, and V. L. Sukhorukov, J. Phys. B **26**, 4381 (1993).
[20] G. Materlik, B. Sonntag, and M. Tausch, Phys. Rev. Lett. **51**, 1300 (1983).
[21] R. Prešeren, A. Kodre, I. Arčon, and M. Borowski, J. Synchrotron Radiat. **8**, 279 (2001).
[22] R. Bruhn, B. Sonntag, and H. W. Wolff, J. Phys. B **12**, 203 (1979).
[23] R. Hauko, J. Padežnik Gomilšek, A. Kodre, I. Arčon, and G. Aquilanti, Radiat. Phys. Chem. **139**, 66 (2017).
[24] S. Bodeur, P. Millié, and I. Nenner, Phys. Rev. A **41**, 252 (1990).
[25] J. Schirmer, A. B. Trofimov, K. J. Randall, J. Feldhaus, A. M. Bradshaw, Y. Ma, C. T. Chen, and F. Sette, Phys. Rev. A **47**, 1136 (1993).
[26] A. P. Hitchcock and C. E. Brion, J. Phys. B **14**, 4399 (1981).
[27] K. C. Prince, L. Avaldi, R. Sankari, R. Richter, M. de Simone, and M. Coreno, J. Electron. Spectrosc. Relat. Phenom. **144**, 43 (2005).
[28] F. Neese, Wiley Interdiscip. Rev.: Comput. Mol. Sci. **2**, 73 (2012).
[29] C. Froese-Fischer, Comput. Phys. Commun. **43**, 355 (1987).
[30] G. Aquilanti, M. Giorgetti, R. Dominko, L. Stievano, I. Arcon, N. Novello, and L. Olivi, J. Phys. D: Appl. Phys. **50**, 074001 (2017).
[31] M. Štuhec, A. Kodre, M. Hribar, D. Glavic-Cindro, I. Arčon, and W. Drube, Phys. Rev. A **49**, 3104 (1994).
[32] A. Filipponi, J. Phys. B **33**, 2835 (2000).
[33] J. A. Bearden and A. F. Burr, Rev. Mod. Phys. **39**, 125 (1967).
[34] M. O. Krause and J. H. Oliver, J. Phys. Chem. Ref. Data **8**, 329 (1979).
[35] A. R. P. Rau and U. Fano, Phys. Rev. **162**, 68 (1967).
[36] U. Fano and J. W. Cooper, Rev. Mod. Phys. **40**, 441 (1968).
[37] M. Stener, G. Fronzoni, D. Toffoli, and P. Decleva, Chem. Phys. **282**, 337 (2002).
[38] M. Stener and P. Decleva, J. Electron. Spectrosc. Relat. Phenom. **94**, 195 (1998).
[39] M. Ya. Amusia, V. K. Ivanov, and V. A. Kupchenko, J. Phys. B **26**, L667 (1981).
[40] M. Ya. Amusia, *Atomic Photoeffect* (Plenum, New York, 1990).
[41] N. M. Novikovskiy, D. V. Rezvan, N. M. Ivanov, I. D. Petrov, B. M. Lagutin, A. Knie, A. Ehresmann, P. V. Demekhin, and V. L. Sukhorukov, Eur. Phys. J. D **73**, 22 (2019).
[42] S. J. Schaphorst, A. F. Kodre, J. Ruscheinski, B. Crasemann, T. Åberg, J. Tulkki, M. H. Chen, Y. Azuma, and G. S. Brown, Phys. Rev. A **47**, 1953 (1993).
[43] V. L. Sukhorukov, A. N. Hopersky, I. D. Petrov, V. A. Yavna, and V. F. Demekhin, J. Phys. **48**, 1677 (1987).
[44] T. A. Carlson and C. W. Nestor, Jr., Phys. Rev. A **8**, 2887 (1973).
[45] T. Mukoyama, Y. Ito, and K. Taniguchi, X-Ray Spectrom. **28**, 491 (1999).
[46] M. Žitnik, M. Kavčič, K. Bučar, A. Mihelič, and R. Bohinc, J. Phys.: Conf. Ser. **488**, 012014 (2014).
[47] M. Kavčič, M. Žitnik, D. Sokaras, T. C. Weng, R. Alonso-Mori, D. Nordlund, J. C. Dousse, and J. Hoszowska, Phys. Rev. A **90**, 022513 (2014).
[48] J. J. Rehr, J. J. Kas, F. D. Vila, M. P. Prange, and K. Jorisen, Phys. Chem. Chem. Phys. **12**, 5503 (2010).
[49] A. D. Becke, Phys. Rev. A **38**, 3098 (1988).
[50] J. P. Perdew, Phys. Rev. B **33**, 8822 (1986).
[51] A. Schaefer, H. Horn, and R. Ahlrichs, J. Chem. Phys. **97**, 2571 (1992).
[52] A. Schaefer, C. Huber, and R. Ahlrichs, J. Chem. Phys. **100**, 5829 (1994).
[53] T. H. Dunning, Jr., J. Chem. Phys. **90**, 1007 (1989).
[54] R. A. Kendall, T. H. Dunning, Jr., and R. J. Harrison, J. Chem. Phys. **96**, 6796 (1992).
[55] R. Püttner, D. Ceolin, R. Guillemin, R. K. Kushawaha, T. Marchenko, L. Journel, M. N. Piancastelli, and M. Simon, Phys. Rev. A **93**, 042501 (2016).
[56] S. H. Southworth, T. LeBrun, Y. Azuma, and K. G. Dyal, J. Electron. Spectrosc. Relat. Phenom. **94**, 33 (1998).
[57] V. G. Yarzhemsky and M. Ya. Amusia, Phys. Rev. A **93**, 063406 (2016).
[58] B. Ravel and M. Newville, J. Synchrotron Radiat. **12**, 537 (2005).
[59] J. C. Slater, Phys. Rev. **36**, 57 (1930).

[60] T. Mukoyama and K. Taniguchi, Phys. Rev. A **36**, 693 (1987).

[61] A. M. Mohammedein, A. A. Ghoneim, J. M. Al-Zanki, M. S. Altouq, and A. H. El-Essawy, Adv. Stud. Theor. Phys. **4**, 55 (2010).

[62] R. Sankari, M. Ehara, H. Nakatsuji, A. De Fanis, H. Aksela, S. L. Sorensen, M. N. Piancastelli, E. Kukk, and K. Ueda, Chem. Phys. Lett. **422**, 51 (2006).

[63] P. W. Atkins and J. de Paula, *Physical Chemistry*, 7th ed. (W. H. Freeman and Company, New York, 2002).